Article

Discovery Medicine 2023; 35(179): 1104–1113
https://doi.org/10.24976/Discov.Med.202335179.107

Bioinspired Synthesis of Ag Nanoparticles onto Polytetrafluoroethylene with Enhanced Antibacterial Activity for Dental Implant Application

He-peng Nie[1,2,3], Qiong Wu[1,2,3], Jin Wu[1,2,3], Kun-zhan Cai[1,2,3], Yue Shen[1,2,3], Chun-bo Tang[1,2,3,*]

[1]Department of Dental Implantology, The Affiliated Stomatological Hospital of Nanjing Medical University, 210029 Nanjing, Jiangsu, China
[2]Jiangsu Province Key Laboratory of Oral Diseases, Nanjing Medical University, 210029 Nanjing, Jiangsu, China
[3]Jiangsu Province Engineering Research Center of Stomatological Translational Medicine, 210029 Nanjing, Jiangsu, China
*Correspondence: cbtang@njmu.edu.cn (Chun-bo Tang)
Published: 1 December 2023

Background: Endosseous implants are widely used as a treatment for tooth loss, but gaps in the implant-abutment interface, and the cavity inside the implant, can cause inflammation of the tissue surrounding the implant. Currently available filling materials, however, cannot solve these problems. Therefore, the development of new antibacterial materials is key. In this study, we synthesized Ag nanoparticle-coated polytetrafluoroethylene (PTFE), analyzed the effect of Ag ion concentration, and estimated the antibacterial effects against oral pathogens *in vitro*.

Method: The Ag nanoparticles (AgNPs)-modified PTFE was achieved using self-polymerized dopamine in an alkaline solution (2 mg/mL) and reduction reaction of Ag ions (0.01 mol/L and 0.05 mol/L). The surface features, chemical components, and wettability were characterized by scanning electron microscopy (SEM), energy-dispersive spectroscopy (EDS), X-ray photoelectron spectroscopy (XPS) and contact angle measurement. The antibacterial effect against *Streptococcus mutans* and *Porphyromonas gingivalis* was evaluated by counting colony-forming units on agar media and the visualization of bacteria present on the specimens by SEM and confocal laser scanning microscope (CLSM).

Results: The surface characterization results indicated that a polydopamine film was successfully formed on the PTFE membrane, and spherical AgNPs were successfully reduced. With increasing concentration of the Ag precursor, the contents of the AgNPs increased ($p < 0.05$). The antibacterial ratio of AgNP-coated PTFE against *Streptococcus mutans* and *Porphyromonas gingivalis* reached 94.2% and 80.6%, respectively. The results of antibacterial testing analyzed via SEM and CLSM also demonstrated the robust antibacterial ability of AgNPs-modified PTFE ($p < 0.05$).

Conclusions: AgNPs-modified PTFE has great potential to function as an implant filling material with enhanced antibacterial properties, and has the potential to be a novel antimicrobial material for the prevention of peri-implantitis in the clinic.

Keywords: antibacterial; dopamine; polytetrafluoroethylene; Ag nanoparticles

Introduction

Although endosseous implants are extensively used as a reliable treatment for tooth loss with high long-term success rates, they are also challenged by peri-implant mucositis and peri-implantitis [1]. These inflammatory conditions are caused by bacterial biofilms that affect the soft and hard tissues around implants [2]. Many studies have shown that gaps at implant-abutment interfaces, and the internal cavity of the implant, serve as channels and reservoirs for bacterial spreading and proliferation, which may cause inflammation of the peri-implant tissues [3]. Different materials such as cotton pellet, gutta-percha, polyvinyl siloxane impression materials, polytetrafluoroethylene (PTFE) tape, and composite resin are used to fill the abutment screw access channels [4]. Other methods and materials such as chlorhexidine gel, GapSeal gel, Oxysafe gel, and Flow.sil are applied to prevent the bacterial leakage. However, a complete hermetic seal cannot be achieved with any of the available sealing agents [5,6]. Thus, there is an urgent need to develop novel antibacterial materials to help solve this problem.

As an implant filling material, PTFE membranes are flexible, minimizing the potential bacterial leakage and creating a better long-term seal. However, the leakage from the abutment-implant interface and the abutment screw access channel cannot be eliminated, and the penetration and colonization of bacteria cannot be prevented entirely [7]. Hence, new dental implant filling materials with antibacterial properties are needed to inhibit microbial attacks. Due to the stable physical and chemical properties and high biocompatibility, PTFE is extensively used in modern implant dentistry [8]. In recent years, many ef-

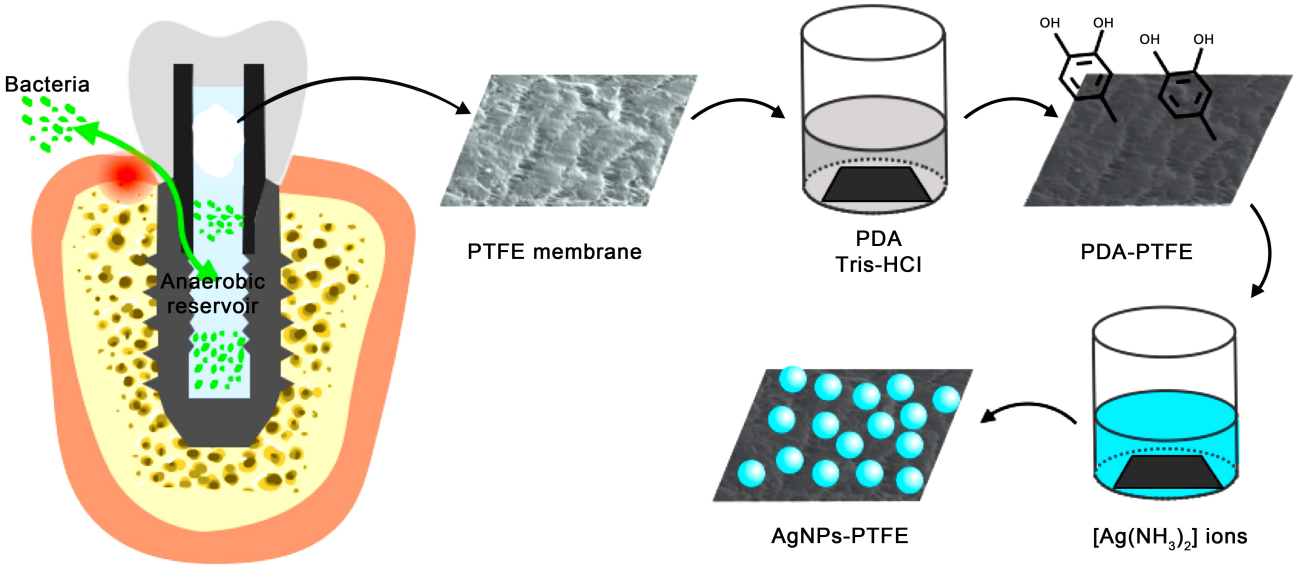

Fig. 1. The schematic of the preparation of AgNPs-PTFE membranes. PTFE, polytetrafluoroethylene; PDA, polydopamine; AgNPs, Ag nanoparticles.

forts have been made to modify the PTFE to inhibit bacterial colonization. Nattharika successfully attached penicillin to expanded PTFE by a series of microwave plasma reactions and esterification reactions [9]. Young grafted a biomembrane-mimic polymer by partial defluorination followed by ultraviolet (UV)-induced polymerization with cross-linkers on the expanded PTFE surface [10]. However, complex methods and expensive equipment are required due to the hydrophobic and chemically inert PTFE surface [11]. Moreover, due to the excessive usage of antibiotics, several pathogens have developed resistance under evolutionary pressure. Thus, the development of antimicrobial compounds to improve antibacterial potential is a priority research area in this modern era.

Recently, Ag nanoparticles (AgNPs) have been highlighted as a promising approach for developing an antibacterial system owing to their effective antibacterial activity and their resilience in developing resistant strains [12–15]. However, the practical applications of AgNPs are hampered by the problem of easy aggregation; the aggregation of the AgNPs will diminish their antibacterial activity. Thus, a synthetic strategy to prepare AgNPs on substrates with excellent antibacterial activity is highly desired. Dopamine, a small molecule with amine and catechol functional groups, can self-polymerize into polydopamine in alkaline pH environments and adhere to any composition [16]. This spontaneous deposition can generate AgNPs *in situ* without other reducing agents [17,18]. Many types of research have proved that an AgNPs layer formed by this method has a promising antibacterial property [19]. However, studies of AgNPs decorated on PTFE against oral pathogens are rare.

In this study, we presented an efficient and straightforward process to induce AgNPs on PTFE. A polydopamine layer was constructed on the hydrophobic PTFE membrane by self-polymerization of dopamine. With abundant amine and catechol groups, the surface of the polydopamine layer reduced the $[Ag(NH_3)_2]^+$ ions *in situ* and fixed the formed AgNPs. The relationship between the concentration of $[Ag(NH_3)_2]^+$ ions and the content of the AgNPs was investigated. Meanwhile, the antibacterial property activity against *Streptococcus mutans* (*S. mutans*) and *Porphyromonas gingivalis* (*P. gingivalis*) was studied on the PTFE membranes. We expect this functional material incorporating AgNPs to have potential in biomedical and clinical applications.

Materials and Methods

Materials

PTFE membranes were kindly provided by College of Materials Science and Technology, Nanjing University of Aeronautics and Astronautics. Dopamine hydrochloride was purchased from Sigma-Aldrich (St. Louis, MO, USA) and used as received. Ag nitrate and aqueous ammonia were purchased from Sinopharm Chemical Reagent Co., Ltd. (Shanghai, China).

Methods

Preparation of AgNPs Coated PTFE

The schematic diagram of the AgNPs-coated PTFE preparation procedure is shown in Fig. 1. PTFE membranes (10×10 mm^2) were cleansed with ethanol and deionized water twice for 15 minutes in an ultrasonic washer. Subsequently, the clean PTFE was submerged in alkaline dopamine solution (2 mg/mL) for 24 hours. The pH was adjusted to 8.5 using a Tris buffer. After rinsing with deion-

ized water, the polydopamine (PDA)-modified PTFE membranes were immersed into $[Ag(NH_3)_2]^+$ ion aqueous solutions for 2 hours. The $[Ag(NH_3)_2]^+$ ion aqueous solution was achieved by adding ammonia dropwise into Ag nitrate solution (0.01 mol/L and 0.05 mol/L). The samples of pristine PTFE, dopamine treated PTFE, 0.01 mol/L and 0.05 mol/L treated PTFE are coded as follows: PTFE, PDA-PTFE, Ag1-PTFE, and Ag5-PTFE, respectively. All specimens were washed in distilled water and kept dry at room temperature until subsequent analysis.

Surface Characterization

Scanning electron microscopy (SEM, Hitachi SU3500, Tokyo, Japan) was employed to evaluate the surface morphology at an accelerating voltage of 15 kV. The samples were dried and sputter-coated with gold for 30 s prior to SEM examination. The SEM facility was also equipped with an energy-dispersive spectrometer (EDS) for chemical analysis. The diameter of AgNPs was measured in two fields selected from three SEM images using ImageJ software (version: 1.8.0, U. S. National Institutes of Health, Bethesda, MD, USA). The EDS was employed for elemental analysis. Surface chemical compositions were also detected using an X-ray photoelectron spectrometer (XPS, ESCALAB 250Xi, Thermo Fisher Scientific, Waltham, MA, USA).

Surface Wettability

The water contact angles of all samples were measured by the sessile drop method using 5 µL water droplet in a contact angle meter (Biolin Theta Flex) at different positions. The average of the three contact angle measurements was calculated for statistical analysis.

Ag Ion Release Test

The total Ag contents of Ag1-PTFE and Ag5-PTFE were measured by sampling (n = 3) in 4% dilute nitric acid. The Ag5-PTFE membranes (n = 3) were immersed in 6 mL of phosphate buffered saline (PBS) at 37 °C to investigate the release behavior of Ag ions every 2 days. The leaching medium was harvested and freshly added at predetermined times (2, 4, 6, and 8 days). Analysis was performed by inductively coupled plasma optical emission spectrometer (ICP-OES, Agilent7500) (Table 1).

Table 1. Surface chemical composition (atom%) of different samples.

Atomic%	C	F	N	O	Ag
PTFE	28.28	71.72	-	-	-
PDA-PTFE	58.05	18.50	6.03	17.43	-
Ag1-PTFE	35.68	16.88	26.48	18.58	2.37
Ag5-PTFE	52.15	14.98	9.09	18.20	5.57

C, Carbon; F, Fluorine; N, Nitrogen; O, Oxygen; Ag, Argentum.

Antibacterial Test *in Vitro*

Gram-positive *Streptococcus mutans* (*S. mutans*, ATCC35668) and Gram-negative *Porphyromonas gingivalis* (*P. gingivalis*, ATCC33277) were used to test antibacterial activity. The bacteria were anaerobically cultured on brain heart infusion (CM1135B, Oxoid, Basingstoke, UK) agar plates supplemented with blood at 37 °C. Colonies from the BHI agar plates were diluted in sterile nutrient broth medium. After 12 h incubation in a constant temperature vibrator at 37 °C with a speed of 200 rpm, both bacterial species at the exponential growth phase were harvested. The bacterial concentrations were adjusted to 10^6 colony-forming units (CFUs)/mL. Then, the specimens (n = 3) were separately incubated with 0.5 mL of the bacteria-containing medium under standard anaerobic conditions. Before bacteria incubation, the specimens were sterilized in an autoclave at 121 °C for 20 minutes.

After being co-cultured for 24 hours, 1 mL of PBS was added and the bacteria on the various specimens were ultrasonically detached for 10 minutes. The bacteria suspensions were serially diluted and re-cultivated on agar plates for colony counting. In this study, bacterial solution co-cultured with PTFE served as the control group. The antibacterial rates were determined by the following relationship: Antibacterial rate (%) = (A – B) / A ×100%, where A is the average CFU count for viable bacteria from PTFE, and B is the CFU count for PDA-PTFE and Ag5-PTFE.

In addition, the bacterial adhesion and morphology were observed by SEM. Briefly, the specimens were gently rinsed with PBS to remove the floating bacteria on the surface, fixed with 3% glutaraldehyde at room temperature overnight, and dehydrated sequentially in a series of ethanol solutions for 10 minutes each. Prior to SEM observation, the specimens were air dried and sputter-coated with gold.

Fluorescence staining was also utilized to distinguish viable/dead bacteria cells, as well as to visualize biofilm formation on the samples after they were co-cultured for 48 hours, using Live/Dead® BacLight™ bacterial viability kits (Invitrogen, ThermoFisher Scientific, Waltham, MA, USA). 500 mL of SYTO (6 µM) and PI (30 µM) staining reagent mixture were added to each sample for 15 minutes in darkness and then examined under confocal laser scanning microscope (CLSM) at XYZ mode.

Statistical Analysis

The quantitative data were presented as means ± standard deviations. One-way analysis of variance was used to compare differences between groups. p values < 0.05 were considered statistically significant.

Results

Surface Characterization

The surface chemical composition of PTFE membranes from different samples is shown in Table 1. The re-

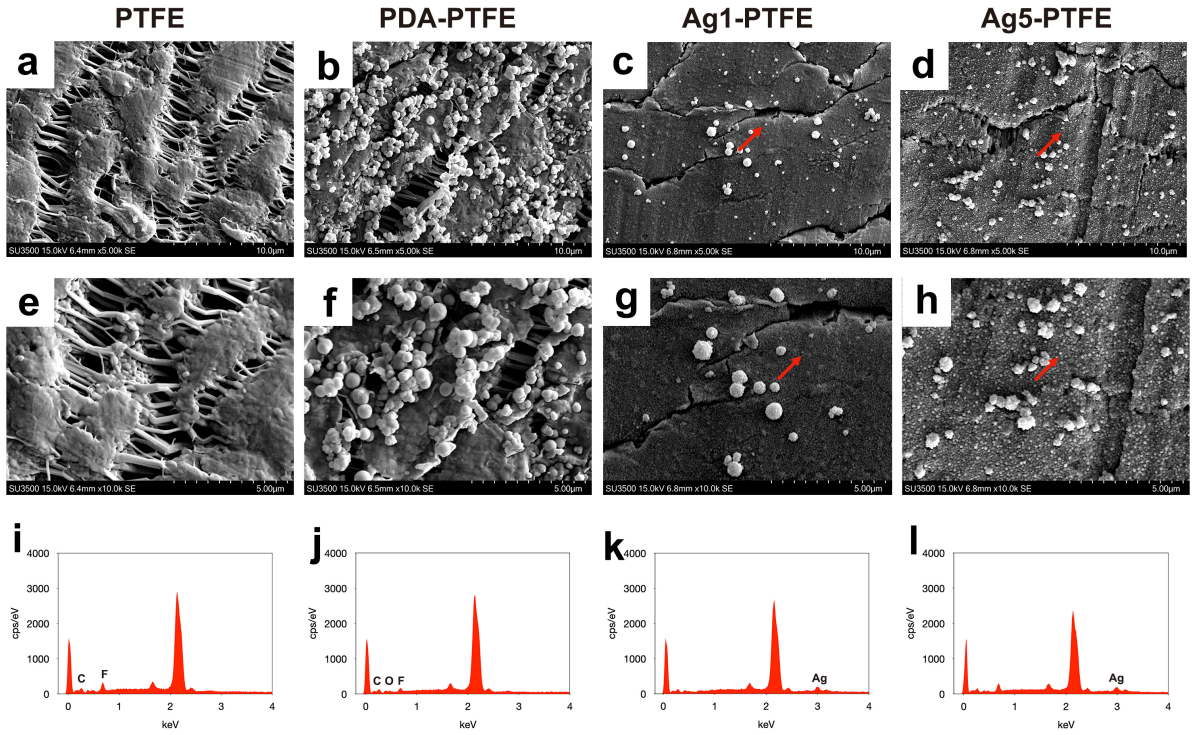

Fig. 2. Morphological characterization and elemental compositions of the different samples. Scanning electron microscopy (SEM) observation for the morphologies of the polytetrafluoroethylene (PTFE) (a,e), polydopamine (PDA)-PTFE (b,f), Ag1-PTFE (c,g) and Ag5-PTFE (d,h). The red arrow showed spherical AgNPs were formed on the surface. The energy-dispersive spectroscopy (EDS) spectra showed the elemental compositions of the PTFE (i), PDA-PTFE (j), Ag1-PTFE (k) and Ag5-PTFE (l) (n = 3).

sults showed that F was the main component of PTFE. The main components of PDA-PTFE were Carbon (C), Fluorine (F), and Oxygen (O). The main components of Ag1-PTFE were C and Nitrogen (N), and a small amount of Ag was also included. The main components of Ag5-PTFE were C, F, and O, with a small amount of Ag.

The surface morphologies of PTFE membranes are shown in Fig. 2. The pristine PTFE membrane presented as a rough surface with a porous structure (Fig. 2a,e), but a thin polydopamine layer was observed on the PDA-PTFE membrane (Fig. 2b,f). In addition, polydopamine particles were randomly deposited on the layer. After immersion into $[Ag(NH_3)_2]^+$ solution, spherical AgNPs covering the polydopamine layer had a diameter of 64.7 $\pm$ 14.2 nm (Fig. 2c,g). When the $[Ag(NH_3)_2]^+$ increased to 0.05 mol/L, as shown in Fig. 2d,h, the deposited AgNPs were larger in size (89.1 $\pm$ 22.8 nm), and the surface was rougher. The EDS spectra showed the elemental compositions of the PTFE, PDA-PTFE, Ag1-PTFE, and Ag5-PTFE (Fig. 2i–l). Carbon and fluorine peaks were detected on the PTFE membrane (Fig. 2i); whereas carbon, oxygen, and fluorine peaks were detected on the PDA-PTFE membrane (Fig. 2j). In addition to carbon, oxygen, and fluorine peaks, Ag peaks were also detected on the Ag1-PTFE and Ag5-PTFE membranes (Fig. 2k,l).

XPS spectroscopy was employed to analyze the surface chemical composition of the membranes. On the wide-scan XPS spectrum of PTFE, C1s and F1s bands are observed (Fig. 3a). On the wide-scanning XPS spectrum, new bands of N1s and O1s attributed to polydopamine were observed for PDA-PTFE (Fig. 3b). In addition, the PDA-PTFE membrane surface displayed a decrease in fluorine atom percentage from 71.72% to 18.50%, and an increase in carbon atom percentage from 28.28% to 58.05% (Table 1), which indicated that more carbon atoms were derived from the polydopamine on the surface. As for Ag5-PTFE, the new signals including Ag3d, Ag3p (Ag3p5/2, Ag3p3/2), and Ag3s were detected in addition to C1s, F1s, N1s, O1s (Fig. 3c). Notably, the XPS core peaks of C1s and Ag3d for Ag5-PTFE were well-fitted. For C1s, the signals at 284.6, 286.0, 287.4, and 292.2 eV were assigned to C–C, C–O, C=O, and CF2 groups, respectively (Fig. 3d). During the polymerization process of dopamine, catechol groups were oxidized into quinone groups (C=O) [20]. For Ag3d, two individual peaks occurred (Fig. 3e). These two characteristic peaks at 367.9 eV and 373.9 eV correspond to the binding energy of Ag 3d5/2 and Ag 3d3/2, respectively. The Ag1-PTFE was also analyzed by XPS, and the results are consistent with Ag5-PTFE. The well-fitted XPS core peaks of Ag3d for Ag1-PTFE were similar to Ag5-PTFE.

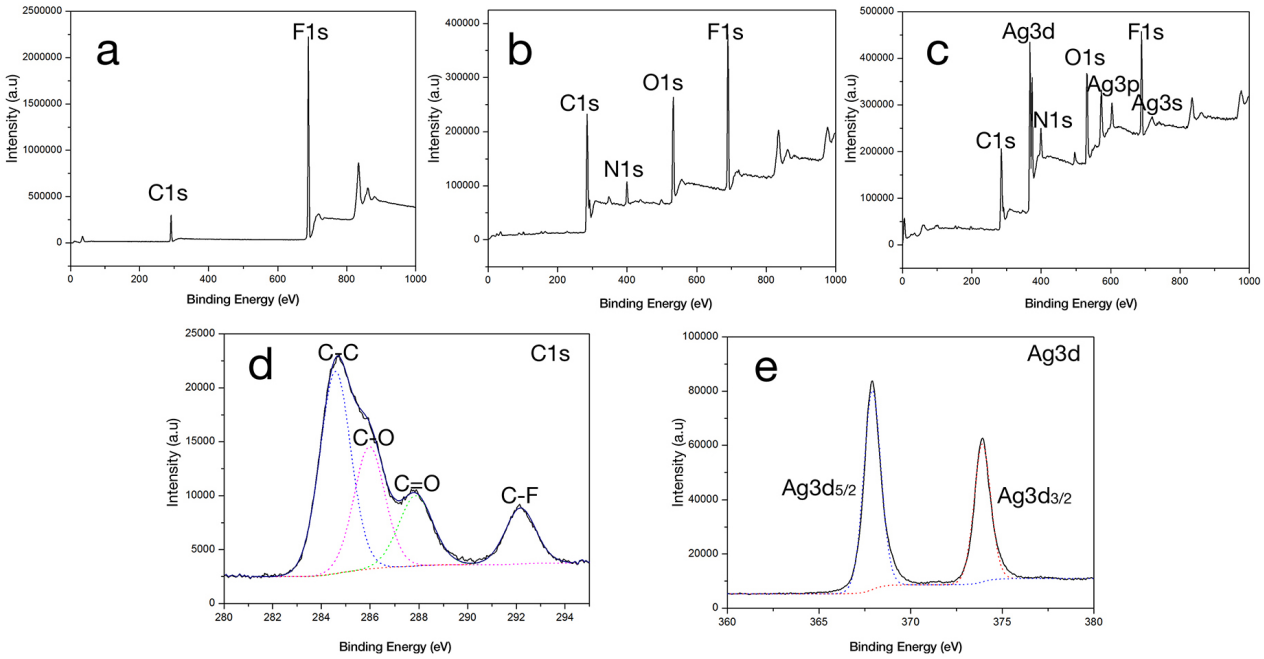

Fig. 3. XPS spectroscopy was employed to analyze the surface chemical composition of the membranes. X-ray photoelectron spectrometer (XPS) spectrum of PTFE (a), PDA-PTFE (b), Ag5-PTFE (c). C1s core level spectra (d) and Ag3d core level spectra (e) of Ag5-PTFE (n = 3).

The split of the doublet in the XPS spectrum of Ag3d is 6.0 eV, indicating that the synthesized Ags were zerovalent. The surface chemical composition (atom%) result detected by XPS is shown in Table 1. Based on these results, we focused on the antibacterial effect of Ag5-PTFE in the follow-up experiment.

Surface Wettability Analysis

The measurement of water contact angle is a common method to characterize the surface wettability. As shown in Fig. 4, the pristine PTFE membrane displayed a hydrophobic property with a contact angle of 127.8 ± 0.7. After being modified by polydopamine, the contact angle decreased to 90.5 ± 1.4 ($p < 0.05$). Subsequently, in situ formation of AgNPs on the PTFE surface further improved the hydrophilicity, and the contact angle decreased to 63.8 ± 6.9 (Ag1-PTFE) and 66.1 ± 5.4 (Ag5-PTFE) ($p < 0.05$).

Ag Ion Release Test

The total Ag contents of Ag1-PTFE and Ag5-PTFE were 16.16 ± 1.42 μg/cm^2 and 22.72 ± 1.46 μg/cm^2, respectively. Ag ions released from Ag5-PTFE were detected at days 2, 4, 6, and 8 in PBS by ICP-OES. In the initial 2 days, a burst release of Ag ions was observed about 6.35 μg/cm^2 (24.2% of total). The liberation of the Ag slowed down with time. The accumulated release amounts were about 14.03 μg/cm^2 (53.5% of total) at 8 days (Fig. 5).

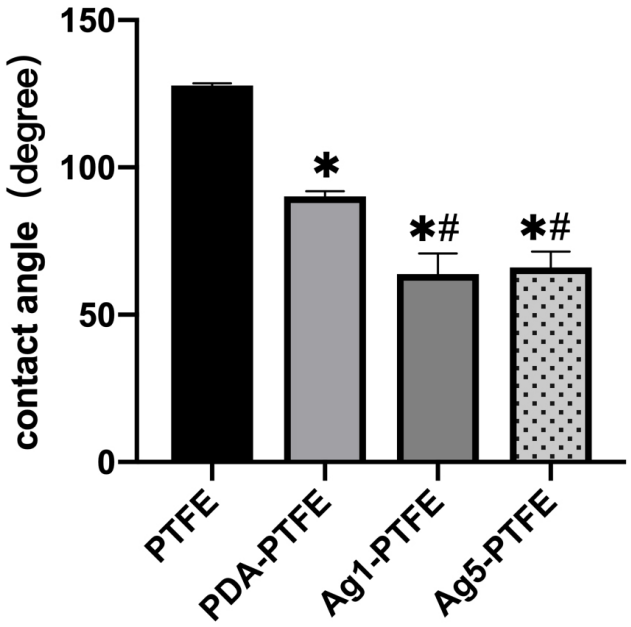

Fig. 4. Surface wettability analysis. * Significantly different from unmodified PTFE, $p < 0.05$; # significantly different from unmodified PDA-PTFE, $p < 0.05$ (n = 3).

Antibacterial Effect

The antibacterial effect of the membranes against *S. mutans* and *P. gingivalis* was examined *in vitro* by incubating them together for 24 hours. The antibacterial property of Ag5-PTFE membrane was quantitatively investi-

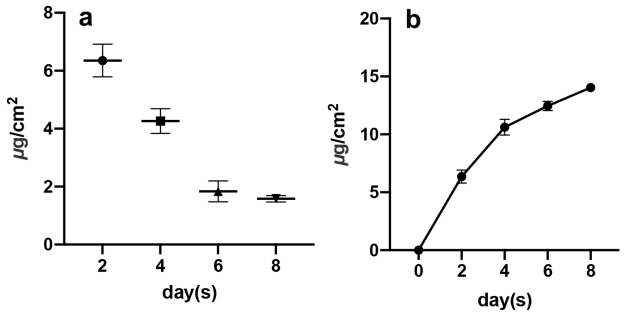

Fig. 5. The total Ag content of Ag1-PTFE and Ag5-PTFE was determined by inductively coupled plasma optical emission spectrometer (ICP-OES) method. (a) Non-cumulative and (b) cumulative release curves of silver ions after immersion at 37 °C at day 2, 4, 6 and 8 (n = 3).

gated through agar plate counting by comparing the average CFU counts of PTFE membranes. As shown in Fig. 6, there were considerably fewer bacterial colonies on the BHI agar plates after a re-culture for the Ag5-PTFE membrane ($p < 0.05$). The antibacterial rate of Ag5-PTFE membrane against *S. mutans* and *P. gingivalis* was 94.2% and 81.8%, respectively. In contrast, both *S. mutans* and *P. gingivalis* colonies were found on the BHI agar plates for PTFE and PDA-PTFE membranes. No obvious decline was seen in the antibacterial rate of PDA-PTFE ($p > 0.05$).

The bacterial adhesion and morphology were observed by SEM. As shown in Fig. 7, there were significant differences between the AgNPs and PTFE. *S. mutans* bacteria on the surface of PTFE and PDA-PTFE membranes were typically rod-shaped, with long chains or large clusters. By contrast, a smaller number of cells adhered to Ag5-PTFE membrane. A similar result was obtained with *P. gingivalis*. In terms of cell morphology, cells on Ag5-PTFE membrane (Fig. 7c,f) displayed an abnormal shape and possible leakage of the intracellular components causing cell damage (the red arrow indicates the fractured cells). In contrast, cells on PTFE and PDA-PTFE membranes (Fig. 7a–e) showed continuous and complete cell membranes.

The live/dead staining of *S. mutans* and *P. gingivalis* was performed to evaluate the antibacterial property of these surfaces. Living and dead bacteria can be distinguished by green and red fluorescence, respectively. As shown in Fig. 8, the surfaces of PTFE and PDA-PTFE membranes supported extensive adherence of *S. mutans* and *P. gingivalis*. Most of the microbial cells on the surfaces were viable (stained green). For the Ag5-PTFE surfaces, a large quantity of dead microbial cells (stained red) was observed, indicating the high efficiency of AgNPs in destroying microbes.

Disccusion

At present, PTFE is widely used in artificial heart valves, vascular grafts, and tissue regeneration patches for its excellent biocompatibility and high physical and chemical stability. Due to the stable surface of PTFE, the materials physically absorbed onto the surface can be easily removed by mechanical shear forces. Moreover, it is challenging to functionalize the C-F bond with other reactive groups [21]. In this research, we introduce a facile, bioinspired route for the functionalization of PTFE membranes. First, the surface of PTFE was modified by mussel-inspired dopamine. It is known that dopamine can self-polymerize and form a multifunctional adhesive layer on various surfaces in aqueous solution. After a multistep reaction of cyclization, oxidation, and rearrangement, a mass of PDA particles was generated in the solution, and a PDA layer was formed on the surface of the substrates [22]. This was confirmed by the appearances of O1s and N1s peaks with high intensities in the XPS scan. Moreover, the C/N mole ratio of PDA-PTFE was 9.6, close to the C/N value of pure dopamine (9.0). These findings indicated that a layer of PDA had been successfully coated on PTFE [23]. Second, taking the polydopamine layer as a powerful platform, Ag nanoparticles were immobilized on the surface. As mentioned, the polydopamine layer has abundant catechol and amine groups. These active groups of polydopamine can chelate with Ag and reduce Ag ions to Ag0. The split of the doublet in the XPS spectrum of Ag3d was 6.0 eV, indicating that the synthesized Ags were zerovalent. The Ag0 was able to bond to the N-site and O-site in polydopamine as a seed precursor. With the continuous reduction of Ag ions, the seed Ags grew to nanoparticles through the addition of atoms [24,25].

The diameter of Ag nanoparticles on the surface increases with the increase in Ag ion concentration. This is similar to the results of Wu [26]. Wu [26] found that when the concentration of $[Ag(NH_3)_2]^+$ ions was low (1.18×10^{-2} mol/L), the Ag nanoparticles on the surface of the material were smaller, with a diameter of 52 nm. With the increase in $[Ag(NH_3)_2]^+$ concentration to 1.96×10^{-2} mol/L, the Ag nanoparticles became larger, with a diameter of about 83 nm. Wang *et al.* [27] also found that the deposited AgNPs were larger and packed more densely with the increasing concentration of Ag ions.

The high contact angle of PTFE may be due to the surface's nonpolar nature, whereas the decreased contact angle indicates the membrane's enhanced hydrophilicity. This result can be explained by the changes in both chemical structure and surface morphology. Massive hydrophilic carboxyl and hydroxyl groups in PDA molecules, in accordance with XPS analysis, can interact with water through Van der Waals' force and hydrogen bonds [28]. The contact angle of AgNPs-modified PTFE was further reduced. According to the aforementioned author's research, the *in-situ*

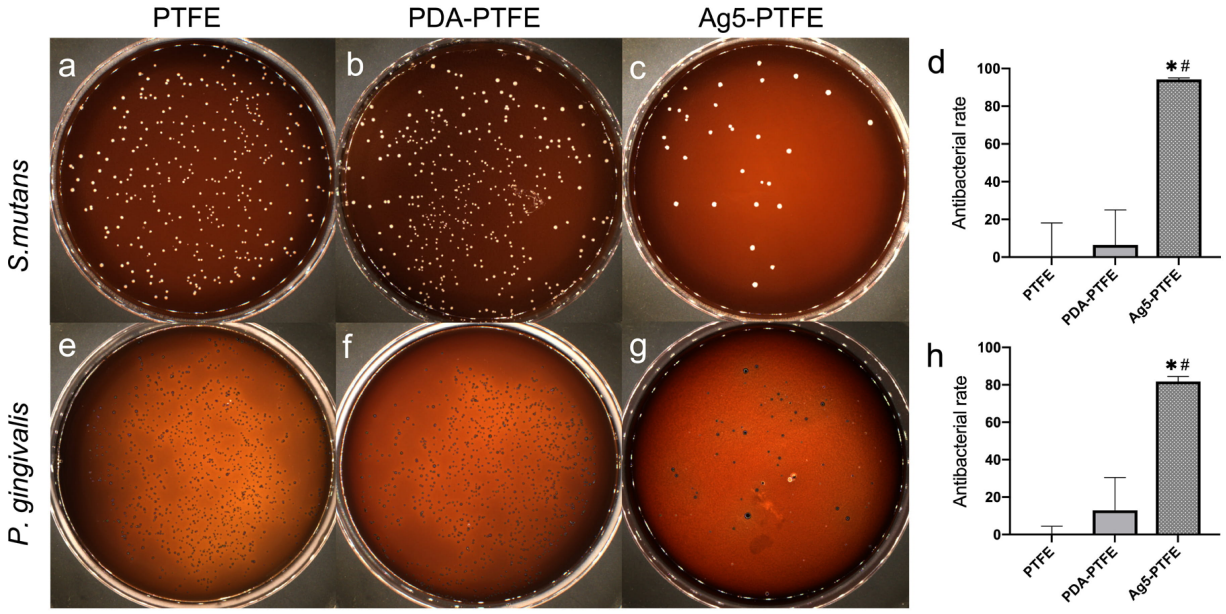

Fig. 6. The detection of viable bacteria suspension from PTFE, PDA-PTFE, and Ag5-PTFE. The antibacterial rate against Gram-positive *Streptococcus mutans* (*S. mutans*) and Gram-negative *Porphyromonas gingivalis* (*P. gingivalis*). (a–c) The effects of PTFE (a), PDA-PTFE (b), and Ag5-PTFE (c) membranes on the bacterial colony of *S. mutans* were observed on the BHI agar plate. (d) The bacterial colony inhibition rate of *S. mutans* was statistically analyzed. (e–g) The effects of PTFE (e), PDA-PTFE (f), and Ag5-PTFE (g) membranes on the bacterial colony of *P. gingivalis* were observed on the brain heart infusion (BHI) agar plate. (h) The bacterial colony inhibition rate of *P. gingivalis* was statistically analyzed. * Significantly different from unmodified PTFE, $p < 0.05$; # Significantly different from unmodified PDA-PTFE, $p < 0.05$ (n = 3).

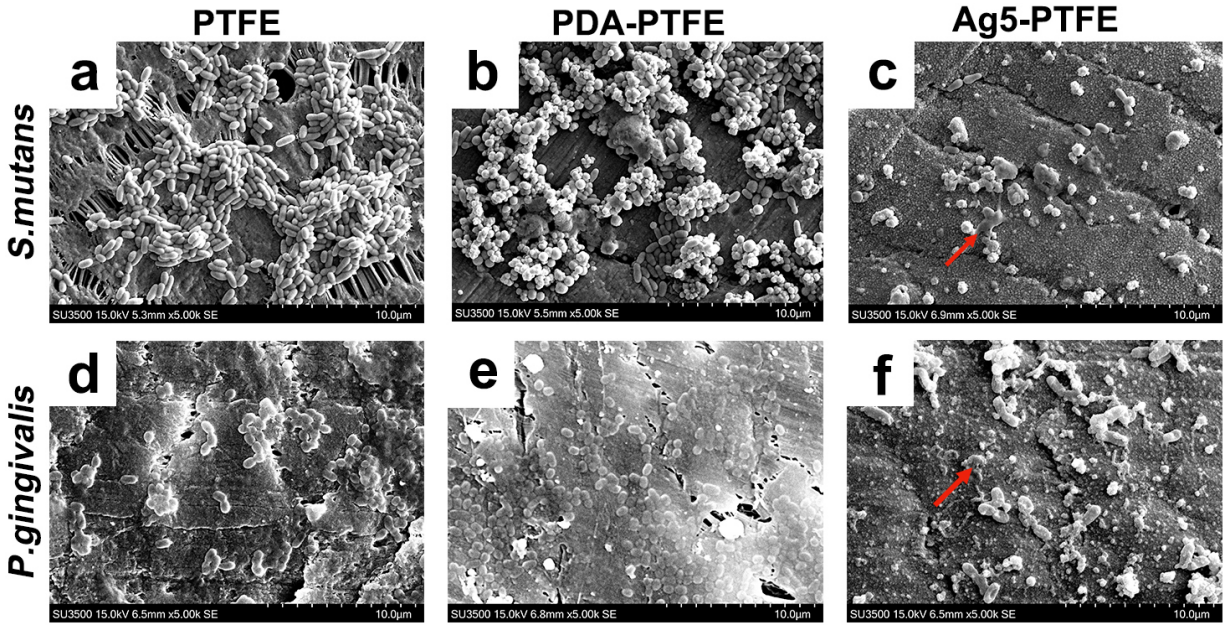

Fig. 7. The attachment and morphological characterization of *S. mutans* and *P.gingivalis* on the different samples. SEM images of *S. mutans* and *P.gingivalis* on PTFE (a,d), PDA-PTFE (b,e), Ag5-PTFE (c,f) (n = 3). The red arrow indicates the fractured cells on the surface.

immobilization of AgNPs can improve the wettability of a membrane surface, due to their hydrophilic nature [29,30].

The AgNPs prepared at the $[Ag(NH_3)_2]^+$ concentration at 0.5 mol/L, which loaded a greater quantity of the Ag ions, were selected to test the antibacterial property. The bacterial strains used in this study were *S. mutans* and *P. gingivalis*. Most other studies have mainly chosen *Escherichia coli* and *Staphylococcus aureus* to test the an-

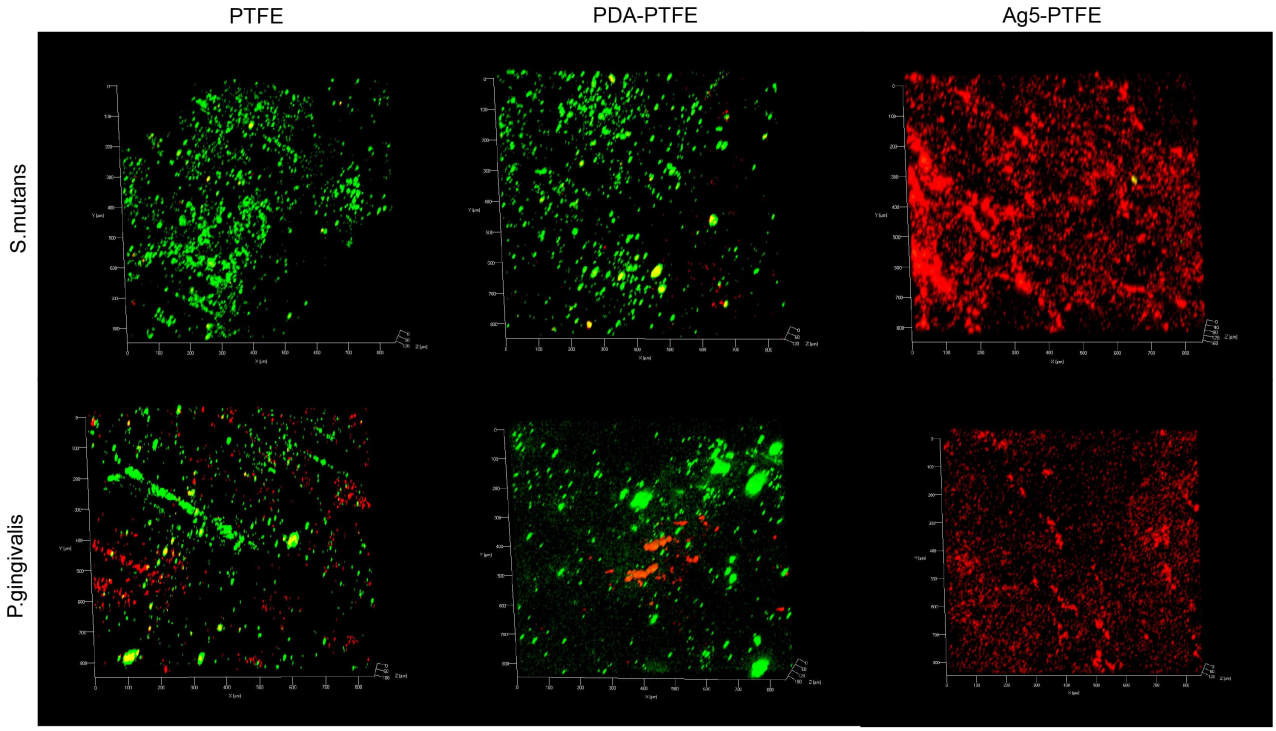

Fig. 8. The 3D confocal laser scanning microscope (CLSM) images of strains grown on specimens, the fluorescence of which includes SYTO (green) for dead cells and PI (red) for live cells.

tibacterial properties of Ag nanoparticles [31,32]. There are relatively few studies on the antibacterial properties of Ag nanoparticles against pathogens for peri-implant mucositis and peri-implantitis. The *S. mutans* and *P. gingivalis* we used in this study are two typical oral pathogens which can be easily detected in the dental implant cavity and play an important role in the etiology and pathogenesis of peri-implant inflammation [33]. It is important to reduce the adhesion and aggregation of pathogens on dental materials. Bacterial adhesion and colonization on the surface play an important role in the antibacterial property of materials. The bacterial adhesion is affected by surface roughness, surface energy and hydrophobicity. It has been demonstrated that the hydrophobic surface facilitates the antibacterial effect. The greater the hydrophobicity is, the more difficult it is to adhere for bacteria. Several studies have reported that bacterial adhesion and colonization greatly reduce on hydrophobic PTFE surfaces [34]. However, other investigations showed that an initial biofilm rapidly accumulates on PTFE surfaces. After being placed in the molar region for 48 hours, Carolina found that the biofilm that formed on the surface of polytetrafluoroethylene was thicker than that of stainless steel [35]. This indicated that relying on the high hydrophobicity of PTFE is not sufficient for antibacterial properties. In this study, numerous bacteria colonizes the hydrophobic surface of the PTFE membrane, whereas the Ag5-PTFE exhibits a contrary result, suggesting that the decoration with AgNPs may be the key reason for the antibacterial effect.

It is well known that Ag and Ag-based nanomaterials have strong antibacterial ability against a variety of bacteria. The exact antibacterial mechanism of AgNPs is still not fully understood. The free Ag ions released from the AgNPs can interact with thiol-containing proteins in the cell wall, inhibiting its function [36,37]. The Ag ions then penetrate through the bacterial wall, leading the DNA molecule to lose its replication ability, which subsequently leads to cell death [38]. Moreover, compared to other salts, the AgNPs display more efficient antibacterial activity due to their large surface-to-volume ratio. The extremely large surface area provides better contact with bacteria, which may allow the particles to attach to the cell membrane and easily penetrate into the microorganisms. In addition, the reactive oxygen species (ROS) generated by Ag ions and AgNPs inhibit the respiratory chain complex enzymes in the bacterial mitochondria, resulting in disruption of ATP production [32,39]. As AgNPs are widely considered a highly-efficient antibacterial agent, its application on the PTFE membrane as an implant filling material appears promising in preventing clinical infection.

However, in order to further develop related products and applications, we still need to conduct *in vivo* research to verify the efficiency and safety of AgNPs-coated PTFE.

Conclusions

In this study, PTFE coated with Ag nanostructures was successfully prepared by a facile method by using poly-

dopamine as a reducing agent. The wettability of the surface significantly improves after polydopamine and AgNPs are coated onto the membrane. Moreover, the AgNPs-coated PTFE membrane exhibits a robust antibacterial activity against oral pathogens *S. mutans* and *P. gingivalis*, an effect attributed to the AgNPs fabricated on the surface. In summary, our findings provide preliminary insights into the development of antibacterial strategies of dental implant filling materials. This study may be helpful for the use of AgNPs to prevent dental implant infection in the future.

Availability of Data and Materials

Data involved in the present work are available from corresponding author upon request.

Author Contributions

HPN and CBT designed the research study. HPN and CBT performed the research. QW, JW, KZC and YS provided help and advice on experiments. QW, JW, KZC and YS analyzed the data. All authors contributed to editorial changes in the manuscript. All authors read and approved the final manuscript. All authors have participated sufficiently in the work and agreed to be accountable for all aspects of the work.

Ethics Approval and Consent to Participate

Not applicable.

Acknowledgment

Not applicable.

Funding

This work was supported by the National Natural Science Foundation of China [grant number 82170993]; The International Science and Technology Cooperation Program of China [grant number 2018YFE0194100]; the Science and Technology Commission Program of Nanjing [grant number 201605011].

Conflict of Interest

The authors declare no conflict of interest.

References

[1] Darby I. Risk factors for periodontitis & peri-implantitis. Periodontology 2000. 2022; 90: 9–12.

[2] Assery NM, Jurado CA, Assery MK, Afrashtehfar KI. Peri-implantitis and systemic inflammation: A critical update. The Saudi Dental Journal. 2023; 35: 443–450.

[3] Sasada Y, Cochran DL. Implant-Abutment Connections: A Review of Biologic Consequences and Peri-implantitis Implications. The International Journal of Oral & Maxillofacial Implants. 2017; 32: 1296–1307.

[4] Jain S. Efficacy of Various Implant Abutment Screw Access Channel Sealing Materials in Preventing Microleakage: A Systematic Review. The Journal of Oral Implantology. 2022; 48: 455–463.

[5] Smojver I, Bjelica R, Vuletić M, Gerbl D, Budimir A, Gabrić D. Antimicrobial Efficacy and Permeability of Various Sealing Materials in Two Different Types of Implant-Abutment Connections. International Journal of Molecular Sciences. 2022; 23: 8031.

[6] Bosquê Keedi C, Azevedo Marques AD, Arenas Rodrigues VA, Avila-Campos MJ, Tortamano P. Efficacy of a Polyglycol Dimethacrylate-Based Adhesive in Sealing the Implant-Abutment Interface. Implant Dentistry. 2019; 28: 265–271.

[7] Rosa EC, Deliberador TM, Nascimento TCDLD, Kintopp CCDA, Orsi JSR, Wambier LM, *et al*. Does the implant-abutment interface interfere on marginal bone loss? A systematic review and meta-analysis. Brazilian Oral Research. 2019; 33: e068.

[8] Moráguez OD, Belser UC. The use of polytetrafluoroethylene tape for the management of screw access channels in implant-supported prostheses. The Journal of Prosthetic Dentistry. 2010; 103: 189–191.

[9] Aumsuwan N, Heinhorst S, Urban MW. Antibacterial surfaces on expanded polytetrafluoroethylene; penicillin attachment. Biomacromolecules. 2007; 8: 713–718.

[10] Jin YJ, Kang S, Park P, Choi D, Kim DW, Jung D, *et al*. Anti-inflammatory and Antibacterial Effects of Covalently Attached Biomembrane-Mimic Polymer Grafts on Gore-Tex Implants. ACS Applied Materials & Interfaces. 2017; 9: 19161–19175.

[11] Tabata Y, Suzuki H, Ikeda S. Radiation modification of PTFE and its application. Radiation Physics and Chemistry. 2013; 84: 14–19.

[12] Ai M, Du Z, Zhu S, Geng H, Zhang X, Cai Q, *et al*. Composite resin reinforced with silver nanoparticles-laden hydroxyapatite nanowires for dental application. Dental Materials: Official Publication of the Academy of Dental Materials. 2017; 33: 12–22.

[13] van Hengel IAJ, Riool M, Fratila-Apachitei LE, Witte-Bouma J, Farrell E, Zadpoor AA, *et al*. Selective laser melting porous metallic implants with immobilized silver nanoparticles kill and prevent biofilm formation by methicillin-resistant Staphylococcus aureus. Biomaterials. 2017; 140: 1–15.

[14] Adnan M, Siddiqui AJ, Ashraf SA, Ashraf MS, Alomrani SO, Alreshidi M, *et al*. Saponin-Derived Silver Nanoparticles from *Phoenix dactylifera* (Ajwa Dates) Exhibit Broad-Spectrum Bioactivities Combating Bacterial Infections. Antibiotics (Basel, Switzerland). 2023; 12: 1415.

[15] Dumlupınar B, Karatoprak GŞ, Fırat M, Akkol EK. Appraisal of the antimicrobial and cytotoxic potentials of nanoparticles biosynthesized from the extracts of *Pelargonium quercetorum* Agnew. Frontiers in bioscience (Landmark Edition). 2021; 26: 1089–1096.

[16] Lee H, Dellatore SM, Miller WM, Messersmith PB. Mussel-inspired surface chemistry for multifunctional coatings. Science (New York, N.Y.). 2007; 318: 426–430.

[17] Faure E, Falentin-Daudre C, Jerome C, Lyskawa J, Fournier D, Woisel P, *et al*. Catechols as versatile platforms in polymer chemistry. Progress in Polymer Science. 2013; 38: 236–270.

[18] Zhu X, Liu H, Wu Y, Ye J, Li Y, Liu Z. Preparation and catalytic properties of polydopamine-modified polyacrylonitrile fibers functionalized with silver nanoparticles. RSC Advances. 2022; 12: 25906–25911.

[19] Deng L, Deng Y, Xie K. AgNPs-decorated 3D printed PEEK implant for infection control and bone repair. Colloids and Surfaces. B, Biointerfaces. 2017; 160: 483–492.

[20] Nardo T, Chiono V, Ciardelli G, Tabrizian M. PolyDOPA Mussel-Inspired Coating as a Means for Hydroxyapatite Entrapment on Polytetrafluoroethylene Surface for Application in Periodontal Diseases. Macromolecular Bioscience. 2016; 16: 288–298.

[21] Schoenbaum TR, Wadhwani C, Stevenson RG. Covering the Implant Prosthesis Screw Access Hole: A Biological Approach to Material Selection and Technique. The Journal of Oral Implantology. 2017; 43: 39–44.

[22] Xu Q, Zhang J, Li X, van Duin DM, Hu Y, van Duin ACT, *et al*. How Polytetrafluoroethylene Lubricates Iron: An Atomistic View by Reactive Molecular Dynamics. ACS Applied Materials & Interfaces. 2022; 14: 6239–6250.

[23] Elbasuney S, El-Sayyad GS. Silver nanoparticles coated medical fiber synthesized by surface engineering with bio-inspired mussel powered polydopamine: An investigated antimicrobial potential with bacterial membrane leakage reaction mechanism. Microbial Pathogenesis. 2022; 169: 105680.

[24] Wu K, Yang Y, Zhang Y, Deng J, Lin C. Antimicrobial activity and cytocompatibility of silver nanoparticles coated catheters via a biomimetic surface functionalization strategy. International Journal of Nanomedicine. 2015; 10: 7241–7252.

[25] Aboelmaati MG, Abdel Gaber SA, Soliman WE, Elkhatib WF, Abdelhameed AM, Sahyon HA, *et al*. Biogenic and biocompatible silver nanoparticles for an apoptotic anti-ovarian activity and as polydopamine-functionalized antibiotic carrier for an augmented antibiofilm activity. Colloids and Surfaces. B, Biointerfaces. 2021; 206: 111935.

[26] Wu C, Zhang G, Xia T, Li Z, Zhao K, Deng Z, *et al*. Bioinspired synthesis of polydopamine/Ag nanocomposite particles with antibacterial activities. Materials Science & Engineering. C, Materials for Biological Applications. 2015; 55: 155–165.

[27] Wang Z, Ou J, Wang Y, Xue M, Wang F, Pan B, *et al*. Antibacterial superhydrophobic silver on diverse substrates based on the mussel-inspired polydopamine. Surface and Coatings Technology. 2015; 280: 378–383.

[28] Li X P, Shan H T, Cao M, Li B. Mussel-inspired modification of PTFE membranes in a miscible THF-Tris buffer mixture for oil-in-water emulsions separation. Journal of Membrane Science. 2018; 555: 237–249.

[29] Yang Z, Wu Y, Wang J, Cao B, Tang CY. In Situ Reduction of Silver by Polydopamine: A Novel Antimicrobial Modification of a Thin-Film Composite Polyamide Membrane. Environmental Science & Technology. 2016; 50: 9543–9550.

[30] Zhao H, Zhang L, Zheng S, Chai S, Wei J, Zhong L, *et al*. Bacteriostatic activity and cytotoxicity of bacterial cellulose-chitosan film loaded with in-situ synthesized silver nanoparticles. Carbohydrate Polymers. 2022; 281: 119017.

[31] Liu L, Cai R, Wang Y, Tao G, Ai L, Wang P, *et al*. Polydopamine-Assisted Silver Nanoparticle Self-Assembly on Sericin/Agar Film for Potential Wound Dressing Application. International Journal of Molecular Sciences. 2018; 19: 2875.

[32] Marassi V, Casolari S, Panzavolta S, Bonvicini F, Gentilomi GA, Giordani S, *et al*. Synthesis Monitoring, Characterization and Cleanup of Ag-Polydopamine Nanoparticles Used as Antibacterial Agents with Field-Flow Fractionation. Antibiotics (Basel, Switzerland). 2022; 11: 358.

[33] do Nascimento C, Pita MS, Calefi PL, de Oliveira Silva TS, Dos Santos JBS, Pedrazzi V. Different sealing materials preventing the microbial leakage into the screw-retained implant restorations: an in vitro analysis by DNA checkerboard hybridization. Clinical Oral Implants Research. 2017; 28: 242–250.

[34] Berry JA, Biedlingmaier JF, Whelan PJ. In vitro resistance to bacterial biofilm formation on coated fluoroplastic tympanostomy tubes. Otolaryngology–head and Neck Surgery: Official Journal of American Academy of Otolaryngology-Head and Neck Surgery. 2000; 123: 246–251.

[35] Fuchslocher Hellemann C, Grade S, Heuer W, Dittmer MP, Stiesch M, Schwestka-Polly R, *et al*. Three-dimensional analysis of initial biofilm formation on polytetrafluoroethylene in the oral cavity. Journal of Orofacial Orthopedics = Fortschritte Der Kieferorthopadie: Organ/official Journal Deutsche Gesellschaft Fur Kieferorthopadie. 2013; 74: 458–467.

[36] Durán N, Durán M, de Jesus MB, Seabra AB, Fávaro WJ, Nakazato G. Silver nanoparticles: A new view on mechanistic aspects on antimicrobial activity. Nanomedicine: Nanotechnology, Biology, and Medicine. 2016; 12: 789–799.

[37] More PR, Pandit S, Filippis AD, Franci G, Mijakovic I, Galdiero M. Silver Nanoparticles: Bactericidal and Mechanistic Approach against Drug Resistant Pathogens. Microorganisms. 2023; 11: 369.

[38] Yin IX, Zhang J, Zhao IS, Mei ML, Li Q, Chu CH. The Antibacterial Mechanism of Silver Nanoparticles and Its Application in Dentistry. International Journal of Nanomedicine. 2020; 15: 2555–2562.

[39] Niyonshuti II, Krishnamurthi VR, Okyere D, Song L, Benamara M, Tong X, *et al*. Polydopamine Surface Coating Synergizes the Antimicrobial Activity of Silver Nanoparticles. ACS Applied Materials & Interfaces. 2020; 12: 40067–40077.